Journal of Power Sources 216 (2012) 290–296

Contents lists available at SciVerse ScienceDirect

Journal of Power Sources

journal homepage: www.elsevier.com/locate/jpowsour

Effect of aqueous electrolytes on the electrochemical behaviors of supercapacitors based on hierarchically porous carbons

Xiaoyan Zhang, Xianyou Wang*, Lanlan Jiang, Hao Wu, Chun Wu, Jingcang Su

Key Laboratory of Environmentally Friendly Chemistry and Applications of Minister of Education, School of Chemistry, Xiangtan University, Hunan, Xiangtan 411105, China

HIGHLIGHTS

- ► Comparable electrochemical performances in various aqueous electrolytes.
- ► In 6.0 M KOH the supercapacitor performs the best electrochemical behaviors.
- ► The highest energy density of the supercapacitor in 6.0 M KOH is 11.54 Wh kg^{-1}.
- ► In 6.0 M KOH the supercapacitor has the shortest relaxation time of 0.62 s.

ARTICLE INFO

Article history:
Received 9 February 2012
Received in revised form
27 March 2012
Accepted 28 May 2012
Available online 1 June 2012

Keywords:
Hierarchically porous carbon
Supercapacitor
Aqueous electrolyte
Electrochemical behaviors

ABSTRACT

Hierarchically porous carbons (HPCs) have been prepared by sol–gel self-assembly technology with nickel oxide and surfactant as the dual template. The porous carbons are further activated by nitric acid. The electrochemical behaviors of supercapacitors using HPCs as electrode material in different aqueous electrolytes, e.g., $(NH_4)_2SO_4$, Na_2SO_4, H_2SO_4 and KOH are studied by cyclic voltametry, galvanostatic charge/discharge, cyclic life, leakage current, self-discharge and electrochemical impedance spectroscopy. The results demonstrate that the supercapacitors in various electrolytes perform definitely capacitive behaviors; especially in 6 M KOH electrolyte the supercapacitor represents the best electrochemical performance, the shortest relaxation time, and nearly ideal polarisability. The energy density of 8.42 Wh kg^{-1} and power density of 17.22 kW kg^{-1} are obtained at the operated voltage window of 1.0 V. Especially, the energy density of 11.54 Wh kg^{-1} and power density of 10.58 kW kg^{-1} can be achieved when the voltage is up to 1.2 V.

1. Introduction

Electrochemical double-layer capacitors (EDLCs) [1] named supercapacitors, with long-cycle life, high power density and reversibility, are a promising energy storage technology for delivering peak power demands in portable electronic application such as electric vehicles. The energy storage of double-layer capacitance relies on the accumulation of charge at electrodes purely by electrostatic, and the charge is separated across the interface between the electrode and the electrolyte [2]. Thus, EDLCs are well suited as backup source because of their low cost and maintenance-free operation. Generally speaking, the electrode materials used the most commonly in EDLCs are carbons due to their high specific surface area of the order of 2500 $m^2\ g^{-1}$. Particularly, hierarchically porous carbons (HPCs) [3] have gained growing interest for the porous texture composed of two or three types of pores which exhibit a great potential for advanced EDLCs applications.

As is well known, the pore size distribution and surface functional groups of carbon materials as well as the size of the electrolyte ions could significantly influence electrochemical performance of supercapacitor. A large number of works [4–6] have been carried out about the electrolytes of EDLCs in various application conditions. There are two principal types of electrolytes in the application of EDLCs, e.g., aqueous and organic electrolytes. For aqueous electrolytes, the acid, alkaline and neutral electrolytes are mostly used due to the advantageously high conductivities and the special mechanism of proton transport. The proton has the highest mobility in an aqueous electrolyte, and its small size allows it to chemisorb to a single oxide ion. As to organic electrolytes, practically, they most often allow operating a supercapacitor to up to 2.3 V based on acetonitrile or propylene carbonate as solvents. The solubility of the salts in the organic solvents is relatively low. If the electrolyte reservoir is too small compared to the large surface of electrodes, the performance of

* Corresponding author. Tel.: +86 731 58292060; fax: +86 732 58292061.
E-mail address: wxianyou@yahoo.com (X. Wang).

0378-7753/$ – see front matter © 2012 Elsevier B.V. All rights reserved.
http://dx.doi.org/10.1016/j.jpowsour.2012.05.090

the supercapacitor is reduced. Since the energy of supercapacitors is proportional to the square of the operating voltage, organic electrolytes are being employed in many commercial EDLCs [7]. However, they have the disadvantages of high internal resistance and electrolyte leakage. Usually, in order to achieve a low ESR of supercapacitors, the high conductivity of current collectors and electrolytes is required and the contact resistance between them should be minimal. Therefore, to develop high performance EDLCs, most of works have been focusing on the aqueous electrolytes. Xia [8] and co-workers have prepared porous carbon electrodes with the specific capacitance of 223 F g^{-1} at 2 mV s^{-1} in 6.0 M KOH electrolyte. Seredych [9] et al. have fabricated supercapacitor electrode based on modified carbons which showed a high specific capacitance of 253 F g^{-1} at 0.05 A g^{-1} in 1.0 M H_2SO_4 electrolyte. Xue [10] and co-workers have reported that supercapacitors in 2.0 M $(NH_4)_2SO_4$ electrolyte with the specific capacitance of 160 F g^{-1} at current density of 10 mA cm^{-2}. Moreover, Demarconnay and coauthors [11] have fabricated supercapacitor in 0.5 M Na_2SO_4 electrolyte with the voltage up to 1.6 V. It is well known that many kinds of electrolytes have been used in the studies of supercapacitors, and different electrolyte for the same an electrode material will give different specific capacitance, so it will be a significant work to discuss the effects of aqueous electrolytes on the electrochemical performance of HPCs.

In previous work, our group have prepared a hierarchically porous carbons (HPCs) by sol–gel self-assembly technology with nickel oxide and surfactant as the dual template [12], and discussed the effects of surfactant template concentration on physical and electrochemical capacitive behaviors [13]. In order to further investigate the adaptability of the hierarchically porous carbons with macro–meso–micro structure in various aqueous electrolytes for different applications, here we will study the supercapacitive performance of hierarchically porous carbon in 2.0 M $(NH_4)_2SO_4$, 2.0 M Na_2SO_4, 0.5 M H_2SO_4, 6.0 M KOH electrolytes.

2. Experimental

2.1. Synthesis of the activated HPCs

Hierarchically porous carbons [12] were prepared by carbonization and corrosion of the dual template precursor. Nickel nitrate hexahydrate ($Ni(NO_3)_2 \cdot 6H_2O$, 98%) and sodium hydroxide (NaOH, 96%) were used as nickel oxide template, and cetyltrimethyl ammonium bromide (CTAB, 99%) dissolved in ethanol-aqueous solutions was used as the surfactant template. The sample with the ratio of dual templates is 4:4. Finally, the resultant carbon was modified by 2 M HNO_3.

2.2. Preparation of the activated HPCs electrodes

As usual in such devices, the electrodes materials for supercapacitors were prepared by mixing 80 wt% activated HPCs with 10 wt% acetylene black and 10 wt% polyvinylidene fluoride (PVDF). After well mixed, the mixtures were blended to obtain slurries. Then the slurries were coated on nickel foams or steel mesh that were used as current collectors and dried in vacuum overnight at 353 K for 12 h. The geometric surface area of the electrodes was kept to be 1.0 cm^2; the electrodes typically had a thickness of about 0.1 mm.

2.3. Evaluation of the electrochemical properties

The electrochemical performances of the as-prepared electrode materials were evaluated by cyclic voltammetry (CV) with scan rates ranging from 1 to 20 mV s^{-1}, galvanostatic charge/discharge (GC) tests at various constant current densities with cutoff voltage of 0.0–1.0 V, electrochemical impedance spectroscopy (EIS) in the frequency range from 10^5 to 10^{-2} Hz with amplitude of 5 mV, leakage current recording the changes of the current at constant voltage state, and self-discharging recording decline of cell voltage (1.0 V) over lengthy periods of time. The CV, GC and EIS measurements were performed by means of electrochemical analyzer systems, CHI660 (CH Instruments, USA). The cycle life, leakage current and self-discharging were measured by potentiostat/galvanostat (BTS 6.0, Neware, Guangdong, China). The aforementioned experiments were carried out using a two-electrode system, named button cell, in which the counter and reference electrodes are the same as the work electrode. The symmetrical button supercapacitors were assembled according to the order of electrode–separator–electrode. And electrolyte solutions of 2.0 M $(NH_4)_2SO_4$, 2.0 M Na_2SO_4, 0.5 M H_2SO_4, or 6 M KOH were used to evaluate the supercapacitors behavior.

3. Results and discussion

Cyclic voltammetries are performed to estimate the electrochemical properties of the symmetric supercapacitors in different electrolytes at the scan rate of 1 mV s^{-1} with the voltage range from 0.0 to 1.0 V. The results are shown in Fig. 1. It can be found that the supercapacitors in their voltage range exhibit similar rectangular capacitive behavior with rapid current responses on voltage reversal at the two end potentials. However, the current response is slower at the two end potentials in 0.5 M H_2SO_4 electrolyte. The supercapacitor in 2 M Na_2SO_4 shows the characteristic CV of an ideal rectangular shape compared with other supercapacitors. It might be inherent to the nature of the Na_2SO_4 electrolyte [11]. The supercapacitor in 6.0 M KOH performs excellent capacitive behavior, and the highest current responses with the potential changing are obtained at the scan rate of 1 mV s^{-1} in Fig. 1. The differences of the current response and CV behaviors for the supercapacitors in various electrolytes are probably attributed to: (I) the ionic radius of the electrolytes, (II) the radius of ionic hydration sphere of electrolytes, (III) the conductivity of the ions and (IV) the mobility of the ions. As well known, the ions would be surrounded by the water of hydration when the water was used as the solvent. Thus, the electric double layers will be built by the ionic hydration sphere of electrolytes. The ionic radius, radius of water of hydration, relative free energy of hydration, molar conductivity and ionic mobility of ions are listed in Table 1 [14–16]. It can be seen from Table 1 that the radius of hydration sphere increases in the order: $H^+ < K^+ = NH_4^+ < Na^+$, and Na^+ ions have larger hydration spheres than other ions because of the $Na^{\delta+}$–$H_2O^{\delta-}$ strong interactions. Nevertheless, the radius of water hydration of all ions is about 2.8–3.8 Å so that the size of the water hydration sphere may not be a deciding factor on electrochemical properties. However, H^+ ions have the higher molar conductivity than other ions, while K^+ and NH_4^+ ions compared to Na^+ ions have distinctly higher molar conductivity due to the mobility of the ions [17]. At the same time, the OH^- ions have the higher molar conductivity than SO_4^{2-} ions. Therefore, the conductivity and mobility of the ions may be the crucial factor on the supercapacitive performance with different electrolytes. For the KOH electrolyte, the molar conductivity of OH^- ions is 198.0 $cm^2\ \Omega^{-1}\ mol^{-1}$. And for the H_2SO_4 electrolyte, the radius of hydration sphere of SO_4^{2-} ions is big but H^+ ions have high molar conductivity of 349.8 $cm^2\ \Omega^{-1}\ mol^{-1}$. Hence, the higher molar conductivity of OH^- and H^+ ions will cause a better supercapacitive behavior. Meanwhile, the NH_4^+ ions in $(NH_4)_2SO_4$ solution have higher conductivity than Na^+ ions in Na_2SO_4 solution, and the H^+ ions produced from hydrolysis of $(NH_4)_2SO_4$ in $(NH_4)_2SO_4$ solution according to Eqs. (1)–(4) will result in the higher current response of the CV in $(NH_4)_2SO_4$ than that in Na_2SO_4 electrolyte.

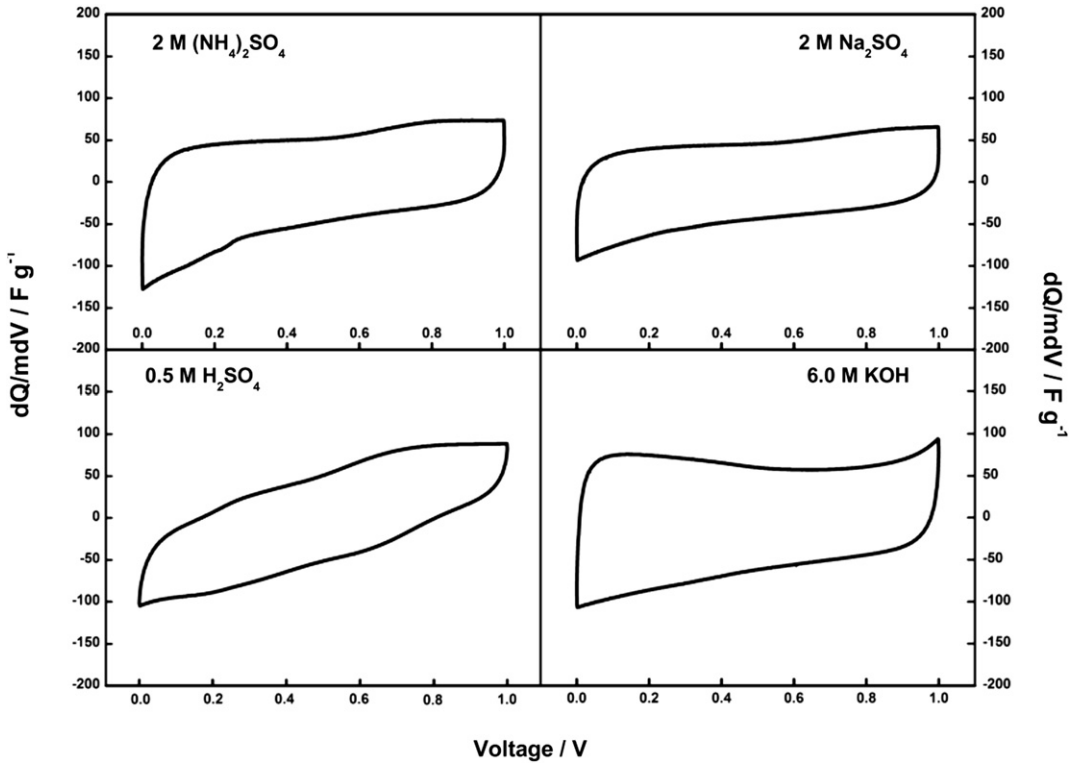

Fig. 1. The CV curves of the supercapacitors in various electrolytes at the scan rate of 1 mV s^{-1}.

$$(NH_4)_2SO_4 = 2NH_4^+ + SO_4^{2-} \quad (1)$$

$$NH_4^+ + OH^- \rightleftharpoons NH_3 \cdot H_2O \quad (2)$$

$$H_2O \rightleftharpoons H^+ + OH^- \quad (3)$$

$$NH_4^+ + H_2O \rightleftharpoons NH_3 \cdot H_2O + H^+ \quad (4)$$

The specific capacitance values of the supercapacitors in different electrolytes can be determined by Eq. (5) [18]:

$$Cs,t = \frac{Ia + |Ic|}{2W(dV/dt)} \quad (5)$$

Where $C_{s,t}$, I_a, I_c, W and dV/dt are the specific capacitance (F g^{-1}), the current (A) of anodic and cathodic voltammetric curves on positive and negative sweeps, the mass of the material (g) (only including the mass of the activated materials, the same below), and the sweep rate (mV s^{-1}), respectively. Table 2 lists the gravimetric specific capacitance (C_g) of the various supercapacitors at 1 mV s^{-1} calculated from Eq. (5) in different electrolytes. The C_g is 49.8, 44.8, 50.6 and 61.5 F g^{-1} for the supercapacitors in 2.0 M $(NH_4)_2SO_4$, 2.0 M Na_2SO_4, 0.5 M H_2SO_4 and 6.0 M KOH, respectively.

Fig. 2 reveals the CV curves of the supercapacitor with electrolyte of 6.0 M KOH at the scan rate from 1 to 20 mV s^{-1}. It can be found from Fig. 2(a) that in 6.0 M KOH the supercapacitor exhibits similar rectangular curves as the scan rate increasing. In addition, extremely sharp current reversals near the potential of 0.0 or 1.0 V are observed in the CV curves at the scan rate of 1–10 mV s^{-1}. Fig. 2(b) shows the specific capacitance *vs*. scan rate. Even at the scan rate of 20 mV s^{-1}, the specific capacitance is still 41 F g^{-1}. Consequently, the above results demonstrate that the hierarchically porous carbon supercapacitor in 6.0 M KOH performs high rate capability.

Typical galvanostatic charge/discharge (GC) curves of the supercapacitors at the current densities from 1 to 5 A g^{-1} in various electrolytes are shown in Fig. 3. The charge/discharge curves of supercapacitors in 2.0 M $(NH_4)_2SO_4$ and 6.0 M KOH electrolyte

Table 1
Crystal radius, radius of hydration sphere, relative free energy of hydration (H^+ aq.:−265 kcal mol^{-1}), molar conductivity and ionic mobility of ions.

Ion	Crystal radius (Å)	Radius of hydration sphere (Å)	Gibbs energy (kcal mol^{-1})	Molar conductivity ($cm^2\ \Omega^{-1}\ mol^{-1}$)	Ionic mobility ($\mu\ 10^{-5}\ cm^2\ s^{-1}\ v^{-1}$)
H^+	–	2.80	0.0	349.8	36.2
K^+	1.33	3.31	179.9	73.5	7.6
Na^+	0.95	3.58	162.3	50.1	5.2
NH_4^+	1.48	3.31	–	73.5	7.6
OH^-	–	3.00	–	198.0	20.6
SO_4^{2-}	–	3.79	–	79.8	8.3

Table 2
The electrochemical properties of the supercapacitors with the hierarchically porous electrode material in different electrolytes.

Electrolyte	Specific capacitance (F g^{-1})				ESR[b] (Ω)	Leakage current (mA)	τ_R (s)
	C_g[a]	C_m[b]	C[c]	C[d]			
2.0 M $(NH_4)_2SO_4$	49.8	35.1	39.1	39.0	5.50	0.10	1.34
2.0 M Na_2SO_4	44.8	33.1	36.9	29.2	6.17	0.03	0.76
0.5 M H_2SO_4	50.6	61.4	46.2	43.6	26.55	0.20	–
6.0 M KOH	61.5	60.9	60.6	57.7	2.83	0.04	0.62

[a] The data calculated from the CV at the scan rate of 1 mV s^{-1}.
[b] The data calculated from the GC at current density of 1 A g^{-1} at the voltage range 0.0–1.0 V.
[c] The data obtained from the cycle life at the voltage range 0.0–1.0 V.
[d] The data obtained from the cycle life at the voltage range 0.0–1.2 V.

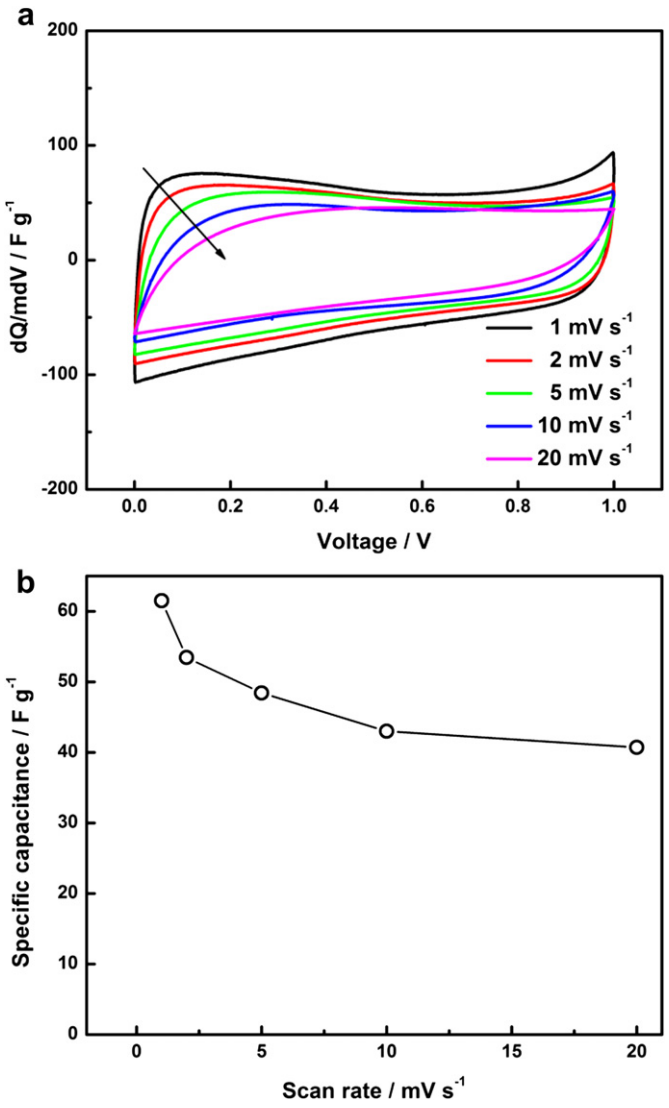

Fig. 2. (a) The CV curves of the supercapacitor in 6.0 M KOH electrolyte at different scan rate from 1 mV s^{-1} to 20 mV s^{-1}. (b) The changes of the specific capacitance with scan rate.

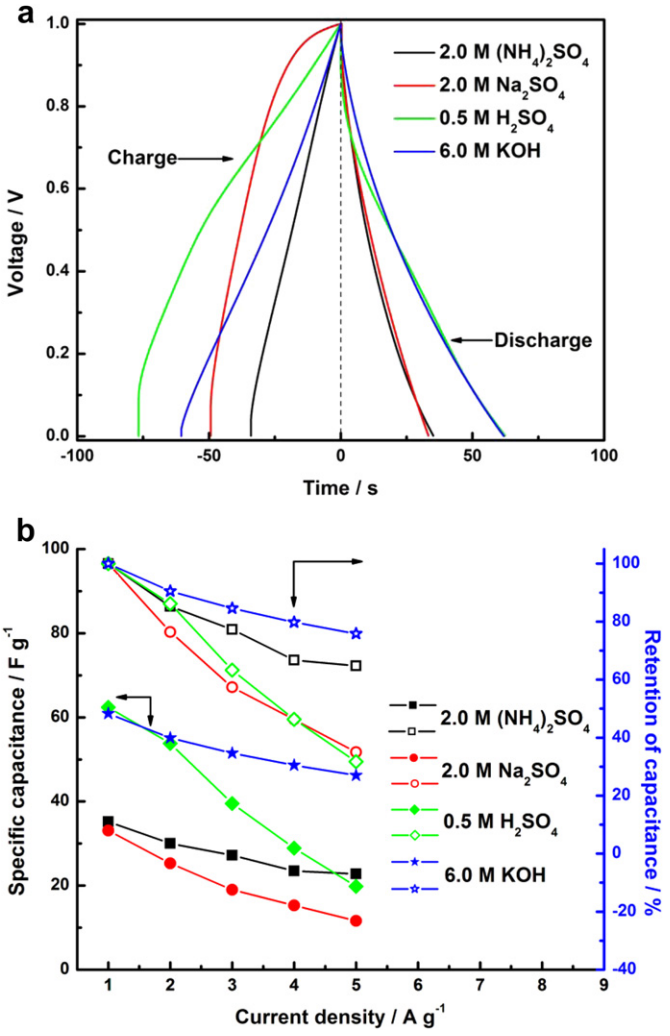

Fig. 3. (a) The GC curves of the supercapacitors in various electrolytes at 1 A g^{-1}. (b) The specific capacitance (■) and GC-SCR (□) of the supercapacitors at different current densities.

solutions at 1 A g^{-1} are almost symmetrical isosceles lines in Fig. 3(a), demonstrating that the supercapacitors in 2.0 M $(NH_4)_2SO_4$ and 6.0 M KOH exhibit high electrochemical capacitive stability. The charge/discharge efficiencies of above two supercapacitors are close to 100%. However, the charge/discharge curves of the supercapacitors in 2.0 M Na_2SO_4 and 0.5 M H_2SO_4 in Fig. 3(a) are asymmetrical isosceles lines. It's due to some pseudo-capacitive redox reactions between the surface functionalities and the aqueous electrolyte [6,19–21]. The specific capacitances of various supercapacitors obtained from the Eq. (6) ref. [22] are listed in Table 2.

$$Cm = \frac{itd}{m\Delta V} \tag{6}$$

Where C_m is the specific capacitance (F g^{-1}), i is the charge/discharge current (A), ΔV is the potential range of the charge/discharge (V), t_d is the discharge time (s), and m is the mass of active material (g) within the electrode. The specific capacitances of various supercapacitors obtained from Eq. (6) at the current density of 1 A g^{-1} are about 35.1, 33.1, 62.4 and 60.9 F g^{-1} for supercapacitors in 2.0 M $(NH_4)_2SO_4$, 2.0 M Na_2SO_4, 0.5 M H_2SO_4 and 6.0 M KOH, respectively. Moreover, Fig. 3(b) compares the specific capacitance and specific capacitance retention (SCR) of the supercapacitors in different electrolytes at various current densities. The specific capacitances of supercapacitor in 6.0 M KOH are the highest and the SCR is 76% even at 5 A g^{-1}. As well known, the power output capability of electrochemical capacitors strongly depends on the equivalent series resistance (ESR) [23]. The ESR is attributed to the resistance of electrolytes and the inner resistance of ion diffusion in mircopore [24], and the values of ESR calculated from the potential drop (IR drop) at the beginning of discharge are listed in Table 2. In 6.0 M KOH the ESR is only 2.83 Ω. Therefore, above results indicate clearly that the supercapacitor in 6.0 M KOH electrolyte can be as high charge/discharge propagation and has good reversibility.

The long-cycle life is one of the most important properties for appliances of supercapacitors. The specific capacitances versus cycle number with constant current charge/discharge cycle at the voltage range from 0.0 to 1.0 V for the supercapacitors in different electrolytes are shown in Fig. 4(a). It is well known that the energy density is directly increased in proportion with the square of voltage. In order to store large amounts of energy, the operated voltage is up to 1.2 V and the results are also exhibited in Fig. 4(a). The supercapacitive and stable properties of the supercapacitors are measured by the steps: (i) 3000 consecutive cycle at 1.0 V, and

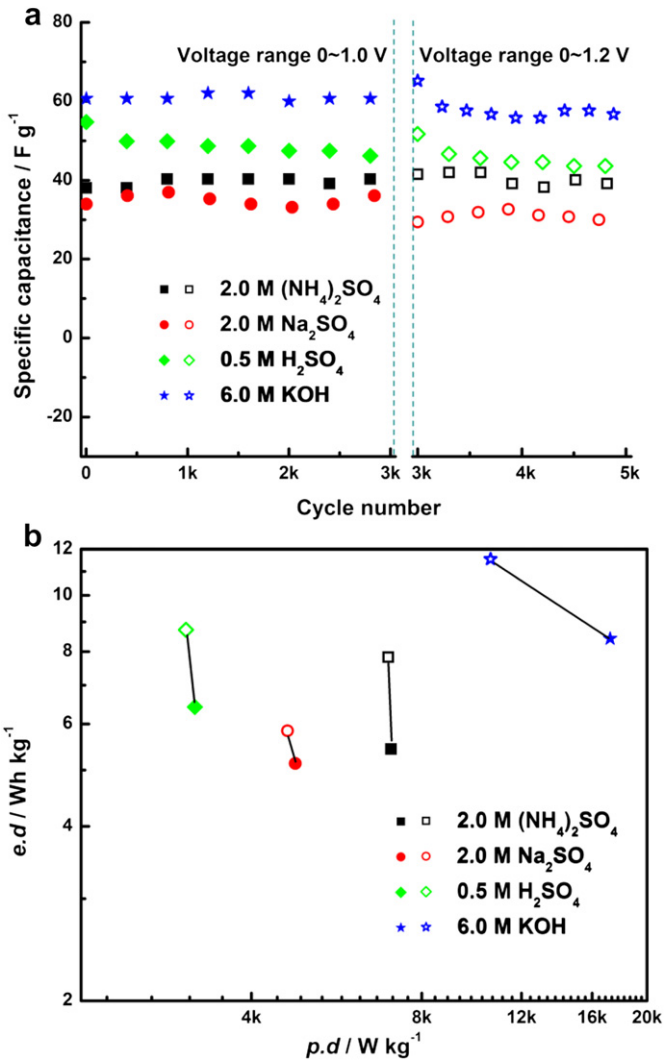

Fig. 4. (a) The cycle life of the supercapacitors in various electrolytes at different voltage range. (b) The Ragone plots of the supercapacitors in various electrolytes with operated voltage of 1.0 V (■) and 1.2 V (□).

then (ii) 2000 consecutive cycle at 1.2 V. The specific capacitances of supercapacitors remain stable for 3000 cycles at 1.0 V in various aqueous electrolytes. However, in 6.0 M KOH the highest specific capacitance of supercapacitor is as high as 60.6 F g^{-1}. When the voltage is up to 1.2 V, the stability of supercapacitor in 0.5 M H_2SO_4 becomes poor because of different overpotential of supercapacitor in different electrolyte leading to occurrence of some decomposition reactions. In 6.0 M KOH the specific capacitance of supercapacitor is high up to 57.7 F g^{-1}. What's more, the energy density (*e.d*) and power density (*p.d*) of the supercapacitors in various electrolytes are calculated from the Eqs. (7) and (8) ref. [25]. And the comparisons of the Ragone plots (*e.d vs. p.d*) of the supercapacitors at the voltage of 1.0 or 1.2 V are shown in Fig. 4(b).

$$E = \frac{1}{2}CV^2 \tag{7}$$

$$P = \frac{V^2}{4mR} \tag{8}$$

Where E is the energy density (Wh kg^{-1}), P is power density (kW kg^{-1}), C is the specific capacitance (F g^{-1}), V is the initial voltage (V), R is the ESR (Ω) and m is the average mass (g) of the two electrodes. At the operated voltage of 1.0 V, the *e.d* of supercapacitors are 5.43, 5.13, 6.42 and 8.42 Wh kg^{-1}, and the *p.d* are 7.06, 4.78, 3.18 and 17.22 kW kg^{-1} for supercapacitors in 2.0 M $(NH_4)_2SO_4$, 2.0 M Na_2SO_4, 0.5 M H_2SO_4 and 6.0 M KOH, respectively. At the same time, when the operated voltage is up to 1.2 V, the *e.d* are 7.82, 5.84, 8.72 and 11.54 Wh kg^{-1}, and the *p.d* are 6.98, 4.64, 3.07 and 10.58 kW kg^{-1} for supercapacitors in 2.0 M $(NH_4)_2SO_4$, 2.0 M Na_2SO_4, 0.5 M H_2SO_4 and 6.0 M KOH, respectively. Obviously, the energy densities of supercapacitors increase as operated voltage up to 1.2 V. Meanwhile, the *e.d* of supercapacitor in 6.0 M KOH electrolyte is distinctly increased with stable cycle life in 1.2 V. Comparatively, KOH solution is a promising electrolyte for HPCs electrode material as supercapacitor in higher operated voltage.

Importantly, the leakage current and self-discharge of supercapacitor are also vital parameters for the application of supercapacitor. Fig. 5 depicts the leakage current and self-discharge curves of supercapacitors in various electrolytes. It can be found from Fig. 5(a) that the leakage current curves of the supercapacitors in different electrolytes drop drastically before 10 min and stay at 0.10, 0.03, 0.20 and 0.04 mA for supercapacitors in 2.0 M $(NH_4)_2SO_4$, 2.0 M Na_2SO_4, 0.5 M H_2SO_4 and 6.0 M KOH, respectively.

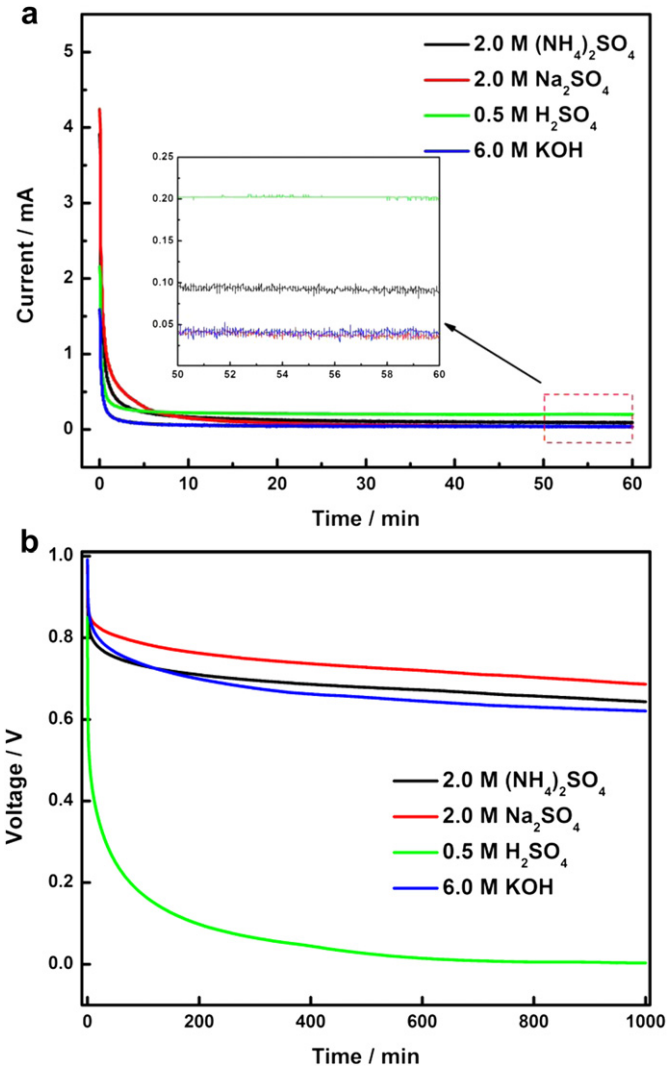

Fig. 5. (a) The leakage current and (b) The self-discharge of the supercapacitors in various electrolytes.

Apparently, lower leakage current implies a higher leakage resistance that causes the supercapacitor to self-discharge slower [26]. Fig. 5(b) presents the self-discharge curves of the supercapacitors in different electrolytes. As a consequence of leakage current, the voltages of supercapacitors reduce gradually with the extending of time, and they decrease quickly before 3 h and become gentle subsequently. Zhou [27] and co-workers have explained this phenomenon as follows: (I) biggish leakage currents and self-discharge are caused when diffusion layer ions regress to bulk solution at the beginning. And then (II) compact layer ions move to diffusion layer because of vibration and concentration difference. As the moving velocity is slow, leakage currents and self-discharge keep relatively jarless and become small after some time. It can be seen from Fig. 5(b) that the supercapacitors show a significant self-discharge and the changes of voltage are small except for supercapacitor in 0.5 M H_2SO_4, and the results are coincide with the leakage currents.

Electrochemical impedance spectroscopy (EIS) results in Fig. 6 provide further evidence of the restriction of the electrolyte ions in the pore networks of carbon electrode material. In the low frequency region, the supercapacitors in aqueous electrolytes except in 0.5 M H_2SO_4 show nearly vertical Nyquist plots because of Warburg impedance in Fig. 6(a), indicating a good capacitive behavior. The deviations from the vertical lines are ascribed to the inner mesopore diffusion, which is strongly dependent on the measured potentials [28]. Moreover, the semi-circles existed in mid-frequency (shown in Fig. 6(a) insert) are a measure of the interfacial charge transfer resistance (R_{ct}) and the double-layer capacitance (C_{dl}) connected in parallel with each other [4]. In the high-frequency region, the first intersection points in the real axis of the Nyquist plots represent the values of the ohmic resistance of the electrolytes and the internal resistance of the electrode material, which is marked as R_s. As the results from Fig. 6(a), the R_s of supercapacitors in various electrolytes are about 1.07, 1.50, 2.65 and 0.77 Ω for supercapacitors in 2.0 M $(NH_4)_2SO_4$, 2.0 M Na_2SO_4, 0.5 M H_2SO_4 and 6.0 M KOH, respectively. Fig. 6(b) reveals Bode plot for the supercapacitors in different electrolytes, indicating response time above 45° phase. It can be seen that in 6.0 M KOH electrolyte the supercapacitor gives the fastest response time. This result suggests that the charge storage contribution of supercapacitor in 6.0 M KOH become fast as an increase in frequency. Moreover, the phase angle is close to 80° (the ideal one should be 90°) at lower frequency limitation, further evidencing the good capacitive property of the supercapacitor in 6.0 M KOH electrolyte.

In EIS measure, the supercapacitors behave as a series combination of a resistance and capacitance and both of them depend on the frequency. In the low frequency region, the capacitance ($C(\omega)$) can be defined as the combination of imaginary of the capacitance ($C''(\omega)$) and real part of the capacitance ($C'(\omega)$), and they can be expressed as following Eqs. (9) and (11) [29,30]:

$$C(\omega) = C'(\omega) + jC''(\omega) \tag{9}$$

$$C'(\omega) = -\frac{Z''(\omega)}{\omega\left|Z(\omega)^2\right|} \tag{10}$$

$$C''(\omega) = \frac{Z'(\omega)}{\omega\left|Z(\omega)^2\right|} \tag{11}$$

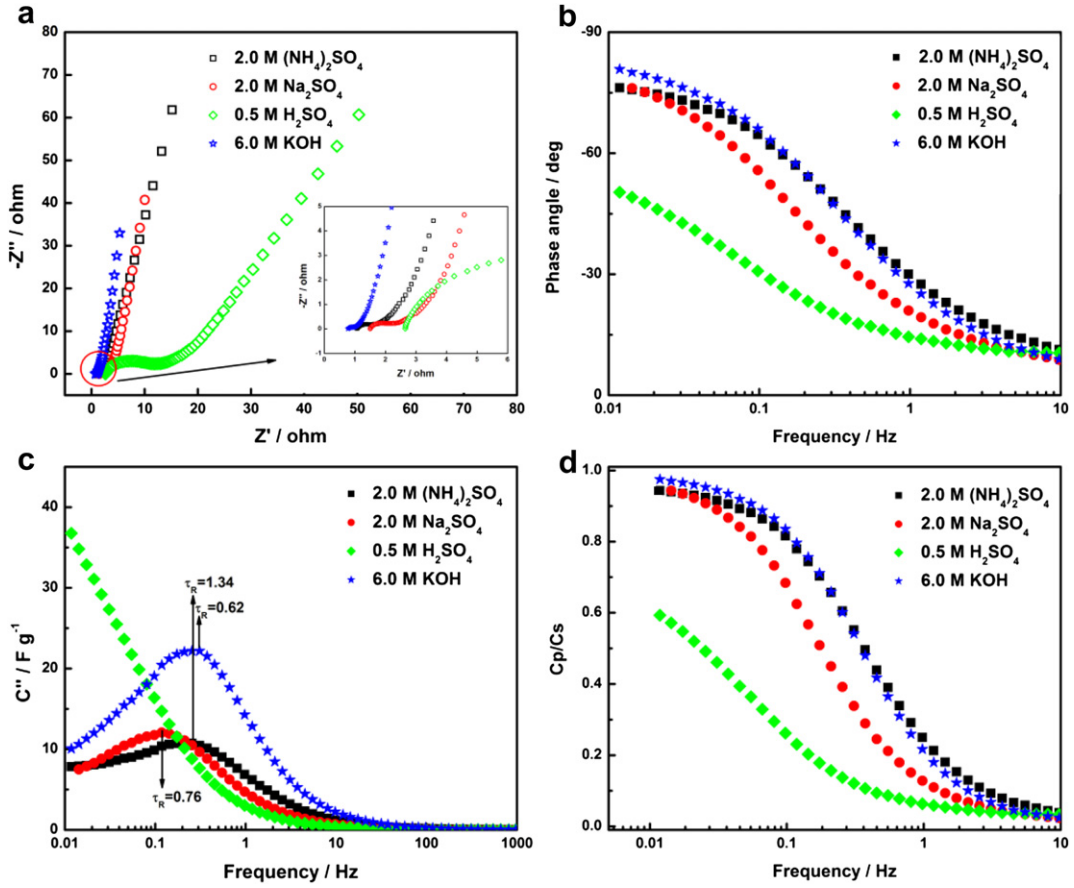

Fig. 6. (a) The Nyquist plots (b) Bode phase angle plots (c) Imaginary capacitance *vs.* frequency dependencies and (d) C_p/C_s *vs.* frequency dependencies of the supercapacitors in different electrolytes.

Where $C'(\omega)$ corresponds to the static capacitance which is tested during the constant current discharge, $C''(\omega)$ corresponds to energy dissipation of the supercapacitor by IR drop and an irreversible faradic charge transfer process, which can cause the hysteresis of the electrochemical processes. $|Z(\omega)|$ is the impedance modulus, and ω is the angular frequency. Moreover, the $C''(\omega)$ versus frequency (f) dependence has a maximum at the so-called relaxation frequency f_R, determining the characteristic time constant RC called relaxation time τ_R. τ_R is a quantitative measure of how fast the device can be charged and discharged reversibly, and it can be expressed by above Eq. (12) [31]:

$$\tau_R = (2\pi f_R)^{-1} \tag{12}$$

Comparison of $C''(\omega)$ *vs.* f plots for various supercapacitors shows that τ_R depends strongly on the electrolyte characteristics. The values of τ_R of the supercapacitors in different electrolytes were given in Table 2. For the supercapacitor in 0.5 M H_2SO_4, τ_R is tiny due to the fast mobility of H^+ ions. However, τ_R of the supercapacitor in 6.0 M KOH is the smallest because of the fast mobility of OH^- ions. Furthermore, the τ_R of supercapacitor with 2.0 M $(NH_4)_2SO_4$ is less than that of supercapacitor with 2.0 M Na_2SO_4 because the mobility of NH_4^+ is larger than that of Na^+.

In addition, the series capacitance values (C_s) at $\omega \to 0$ and the parallel capacitance (C_p) can be calculated according to the following Eqs. (13) and (14) [30], and the dependence of the C_p/C_s ratio on frequency are displayed in Fig. 6(d).

$$C_s = (j\omega Z'')^{-1} \tag{13}$$

$$C_p = \frac{Z''}{|Z|^2\omega} \tag{14}$$

For the ideally polarization system, $C_p/C_s = 1$. According to the Fig. 6(d), the ratio values C_p/C_s for the supercapacitors in various electrolytes approximate to 1.0 except in 0.5 M H_2SO_4. The smallest deviation of C_p/C_s about 0.03 from 1.0 in low frequency is observed for supercapacitor in 6.0 M KOH solution, indicating a nearly ideal polarisability.

4. Conclusion

Cyclic voltammetry, galvanostatic charge/discharge, cyclic life, leakage current, self-discharge and electrochemical impedance spectroscopy methods have been used to compare the electrochemical behaviors for the supercapacitors based on the hierarchically porous carbons electrode material in 2.0 M $(NH_4)_2SO_4$, 2.0 M Na_2SO_4, 0.5 M H_2SO_4, or 6 M KOH electrolyte solutions, respectively. The analysis results reveal that the supercapacitor in 6.0 M KOH electrolyte performs the best electrochemical behaviors, the most excellent reversibility and nearly ideal polarisability. The highest specific capacitance of supercapacitor in 6.0 M KOH observed from CV at the scan rate of 1 mV s^{-1} is 61.5 F g^{-1}. The smallest ESR and R_s is 2.83 Ω and 0.77 Ω. Moreover, the supercapacitor in 6.0 M KOH electrolyte displays the most stable cyclability even at the operated voltage up to 1.2 V, and has the shortest relaxation time of 0.62 s. In addition, the *e.d* and *p.d* of the supercapacitor in 6.0 M KOH is about 8.42 Wh kg^{-1} and 17.22 kW kg^{-1} at the operated voltage window of 1.0 V, and about 11.54 Wh kg^{-1} and 10.58 kW kg^{-1} when the voltage is high up to 1.2 V. Therefore, it can be concluded that the 6.0 M KOH aqueous solution is a promising electrolyte to be used in the supercapacitor with activated HPCs as electrode material.

Acknowledgements

This work was financially supported by the National Natural Science Foundation of China (Grant No. 51072173), Specialized Research Fund for the Doctoral Program of Higher Education (Grant No. 20094301110005), the Scientific Research Fund of Hunan Provincial Education Department (Grant No. 11C1210).

References

[1] B.E. Conway, Electrochemical Supercapacitors: Scientific Fundamentals and Technological Applications, Kluwer Academic/Plenum Publishing, New York, 1999.
[2] T.E. Rufford, D. Hulicova-Jurcakova, E. Fiset, Z. Zhu, G.Q. Lu, Electrochem. Commun. 11 (2009) 974–977.
[3] D.W. Wang, F. Li, M. Liu, G.Q. Lu, H.M. Cheng, Angew. Chem. Int. Ed. 47 (2008) 373–376.
[4] Q.T. Qu, B. Wang, L.C. Yang, Y. Shi, S. Tian, Y.P. Wu, Electrochem. Commun. 10 (2008) 1652–1655.
[5] A. Lewandowski, M. Zajder, E. Frąckowiak, F. Béguin, Electrochim. Acta 46 (2001) 2777–2780.
[6] M.P. Bichat, E. Raymundo-Pinñero, F. Béguin, Carbon 48 (2010) 4351–4361.
[7] A.G. Pandolfo, A.F. Hollenkamp, J. Power Sources 157 (2006) 11–27.
[8] K. Xia, Q. Gao, J. Jiang, J. Hu, Carbon 46 (2008) 1718–1726.
[9] M. Seredych, D. Hulicova-Jurcakova, G.Q. Lu, T.J. Bandosz, Carbon 46 (2008) 1475–1488.
[10] Y. Xue, Y. Chen, M.L. Zhang, Y.D. Yan, Int. J. Min. Met. Mater. 16 (2009) 112–118.
[11] L. Demarconnay, E. Raymundo-Piñero, F. Béguin, Electrochem. Commun. 12 (2010) 1275–1278.
[12] X.Y. Zhang, X.Y. Wang, Y.S. Bai, X.Y. Wang, J.C. Su, J. Electrochem. Soc. 159 (2012) A431–A437.
[13] X.Y. Zhang, X.Y. Wang, J.C. Su, X.Y. Wang, L.L. Jiang, H. Wu, C. Wu, J. Power Sources 199 (2012) 402–408.
[14] B. Tansel, J. Sager, T. Rector, J. Garland, F. Richard, S.L. Levine, M. Roberts, M. Hummerick, J. Bauer, Sep. Purif. Technol. 51 (2006) 40–47.
[15] R.D. Shannon, Acta Cryst. A32 (1976) 751–767.
[16] R.S. Berry, S.A. Rice, J. Ross, Physical Chemistry, second ed. John Wiley & Sons, Inc, 1980.
[17] R.N. Reddy, R.G. Reddy, J. Power Sources 124 (2003) 330–337.
[18] C.C. Hu, C.C. Wang, Electrochem. Commun. 4 (2002) 554–559.
[19] B. Erable, N. Duteanu, S.M.S. Kumar, Y. Feng, M.M. Ghangrekar, K. Scott, Electrochem. Commun. 11 (2009) 1547–1549.
[20] X. Lu, H. Dou, B. Gao, C. Yuan, S. Yang, L. Hao, L. Shen, X. Zhang, Electrochim. Acta 56 (2011) 5115–5121.
[21] I.Y. Jang, H. Muramatsu, K.C. Park, Y.J. Kim, M. Endo, Electrochem. Commun. 11 (2009) 719–723.
[22] Y.G. Wang, H.Q. Li, Y.Y. Xia, Adv. Mater. 18 (2006) 2619–2623.
[23] R. Kötz, M. Carlen, Electrochim. Acta 45 (2000) 2483–2498.
[24] H. Teng, Y.J. Chang, C.T. Hsieh, Carbon 39 (2001) 1981–1987.
[25] E. Raymundo-Piñero, F. Leroux, F. Béguin, Adv. Mater. 18 (2006) 1877–1882.
[26] C. Masarapu, H.F. Zeng, K.H. Hung, B. Wei, ACS Nano 3 (2009) 2199–2206.
[27] S.Y. Zhou, X.H. Li, Z.X. Wang, H.J. Guo, W.J. Peng, Trans. Nonferrous Met. Soc. China 17 (2007) 1328–1333.
[28] W. Sugimoto, H. Iwata, K. Yokoshima, Y. Murakami, Y. Takasu, J. Phys. Chem. B 109 (2005) 7330–7338.
[29] J. Eskusson, A. Jänes, A. Kikas, L. Matisen, E. Lust, J. Power Sources 196 (2011) 4109–4116.
[30] H. Kurig, A. Jänes, E. Lust, J. Electrochem. Soc. 157 (2010) A272–A279.
[31] D. Wang, W. Ni, H. Pang, Q. Lu, Z. Huang, J. Zhao, Electrochim. Acta 55 (2010) 6830–6835.